LATERALLY AVERAGED 2D MODEL FOR THERMAL STRATIFICATION SIMULATIONS IN RESERVOIR ENVIRONMENTS

Leon Matos Ribeiro de Lima, matosleon@gmail.com
Norberto Mangiavacchi, norberto.mangiavacchi@gmail.com
Universidade do Estado do Rio de Janeiro
Rua Fonseca Teles, 121, São Cristovão, Rio de Janeiro, RJ

José da Rocha Miranda Pontes, jopontes@metalmat.ufrj.br
Universidade Federal do Rio de Janeiro
Av. Pedro Calmon, 550, Cidade Universitária, Rio de Janeiro, RJ

João Fontoura, joao.fontoura@promon.com.br
Promon Engenharia
Praia do Flamengo, 154, Flamengo, Rio de Janeiro, RJ

Abstract. *Many environmental impacts associated to hydroelectric reservoir filling processes depend strongly on the depth in the aquatic body, such as thermal and hydraulic stratifications, which can lead to formation of layers of different oxygen concentrations, affecting decomposition of drown organic material. 2d approaches are often more indicated for several environmental flows than 3d models because, for many applications, they provide predictions of adequate accuracy in a very short processing time compared to the respective 3d simulation (actually one order of magnitude shorter). In the specific case of hydroelectric reservoirs, the appropriate 2d model is derived by integrating across the reservoir, which leads to the laterally averaged equations of motion. In this paper, a 2dw model (laterally averaged model, w coming from width, analogous to 2dh model) applied to hydroelectric reservoir hydrodynamic simulations will be presented, focusing on the analysis of thermal stratification. To arrive at the 2dw equations, the 3d equations of momentum and mass conservation for incompressible flow and the transport equation were integrated over the width. The resulting PDE's system is numerically solved by the Finite Element Method and the domain is discretized in a triangular finite element mesh, with the Galerkin Method employed to approximate the node values of velocity components, pressure and temperature. The convective terms were time discretized according to the Semi-Lagrangian scheme. These implementations give rise to an algebraic linear system, which is solved by the preconditioned conjugate gradient method. Mass flux due to evaporation is regarded as boundary condition on the water surface, while non slip boundary condition is set for the bottom. Boussinesq approximation is applied to Navier-Stokes equations, allowing density currents to be captured by the model. Beyond presenting the 2dw equations and the numerical model, this paper also shows a comparison between results obtained by 2dw simulations and experimental results for a lock-exchange problem.*

Keywords: *laterally averaged 2d model, thermal stratification, environmental flows, Finite Element Method, hydroelectric reservoir*

1. INTRODUCTION

Hydroelectric reservoirs are related to many environmental phenomena which are strongly dependent on the depth, such as thermal and/or hydraulic stratification and organic material transport. The changes of the main parameters associated to these problems along the reservoir depth are much more significant than the changes along the horizontal planes.

The low velocities predominating in the reservoir hydrodynamics – which is why many times the hydroelectric reservoir is referred to as lake – are a favorable factor for the formation of thermal stratification, making it a common phenomenon in such environments. Additionally, thermal stratification is influenced by other variables, and can sometimes be broken, causing many perturbations in local ecosystems. Thermal stratification results in the accumulation of poor quality water in the bottom, many times in anaerobic conditions, configuring a region of low oxygen concentrations and high acidity. Wind and low temperatures at the lake surface, for instance, may act to brake the stratification, pushing the bad quality water to the top, causing negative ecological impacts that influences local fauna and fauna downstream of the dam. Many times, specially in deep reservoirs, the stratification acts as a barrier against the water from the bottom and is controlled to avoid that it breaks.

Another issue of main importance in reservoir environments is the transport of organic material and the BOD-DO balance. BOD (biochemical oxygen demand) is an equivalence of vegetable mass density on the aquatic phase in oxygen demand, while DO (dissolved oxygen) is a balance of the oxygen absorbed by the aquatic system due to reareation (surface

O_2 inflow) and organic decomposition (O_2 consumption), which is proportional to BOD concentration. The BOD-DO balance in hydroelectric reservoir filling processes is associated with the hydrodynamic behavior, and this coupling is in the core of discussions about ecological equilibrium of lakes and reservoirs.

Thus, models for predictions on ambient impacts play an increasing role on the study and control of ecological systems wealth, especially in environments with human alterations. The objective of water quality models as management tools is much accentuated in systems that suffer anthropogenic influence [Jorgensen, 1979]. The interactions between hydrodynamic effects and thermal phenomena or organic matter distributions rely in the transport of such variables. Mathematical models for water bodies like reservoirs can be classified taking into account the number of space dimensions, such as 3d, 2d, 1d and 0d. 3d models are the more sophisticated and complex, yet the more expensive to run in terms of computational costs. 2d approaches are often more indicated for several environmental flows than 3d models because, for many applications, it provides predictions of adequate accuracy in a very short processing time compared to the respective 3d simulation (actually one order of magnitude shorter). In the specific case of hydroelectric reservoirs, the most appropriate 2d model is derived by integrating across the reservoir [Karpik and Raithby, 1990], which leads to the laterally averaged equations of motion.

This paper presents a laterally averaged model applied to hydroelectric reservoir hydrodynamic simulations and temperature/concentration transport to predict effects of thermal stratification and distribution of chemical parameters. The solution of the PDE's system is approximated by the Finite Element Method, using triangular meshes for domain discretization. More details on the numerical scheme will be addressed along this paper. Comparisons between experimental and simulation results of a gravity currents problem will be shown as a stage of code validation. Additionally, simulation results of a hydroelectric reservoir problem will be presented to illustrate the model applicability.

2. MATHEMATICAL MODEL

The equations that constitute the model are obtained by laterally integrating the Navier-Stokes equation, the continuity equation (assuming incompressible flow) and the transport equation, as follows

$$\int_B \left[\rho \frac{D\hat{\mathbf{v}}}{Dt} - \nabla \cdot \underline{\mathrm{T}} - \rho \mathbf{g}\right] db = 0; \tag{1}$$

$$\int_B \left[\nabla \cdot \hat{\mathbf{v}}\right] db = 0 \tag{2}$$

$$\int_B \left[\frac{D\hat{c}}{Dt} - \nabla \cdot (D \nabla \hat{c})\right] db = 0 \tag{3}$$

In the above equations the del operator, represented by ∇, is used as divergent and gradient operators. The velocity field is represented by $\hat{\mathbf{v}}$ and $\hat{c}$ is a scalar field, which can be temperature or a certain concentration. $\underline{\mathrm{T}}$ is the Cauchy stress tensor, ρ is the density, $\mathbf{g}$ represents the gravity acceleration, given by $\mathbf{g} = g\mathbf{k}$, where g is the modulus of gravity acceleration, and D is the diffusivity coefficient. B represents the local width. The three coordinate directions are denoted by s (longitudinal direction), z (vertical direction) and b (lateral direction). That is why the integration element in the above equations is db. More details about the concept of these coordinates will be explained ahead. After integrating, and taking into account that the stress tensor is given by

$$\underline{\mathrm{T}} = \begin{bmatrix} \tau_{ss} & \tau_{sz} & \tau_{sb} \\ \tau_{zs} & \tau_{zz} & \tau_{zb} \\ \tau_{bs} & \tau_{bz} & \tau_{bb} \end{bmatrix} \tag{4}$$

we arrive at the 2d laterally averaged equations of motion and transport (in its dimensionless form, expanded in s and z coordinates):

$$\frac{\partial u}{\partial t} + u\frac{\partial u}{\partial s} + w\frac{\partial u}{\partial z} = \frac{1}{\rho B Re}\left[\frac{\partial (B\tau_{ss})}{\partial s} + \frac{\partial (B\tau_{zs})}{\partial z}\right] + \frac{1}{\rho B}\left(\tau_s^L + \tau_s^R\right) \tag{5}$$

$$\frac{\partial w}{\partial t} + u\frac{\partial w}{\partial s} + w\frac{\partial w}{\partial z} = \frac{1}{\rho B Re}\left[\frac{\partial (B\tau_{zs})}{\partial s} + \frac{\partial (B\tau_{zz})}{\partial z}\right] + \frac{1}{\rho B}\left(\tau_z^L + \tau_z^R\right) + g \tag{6}$$

$$\frac{\partial (Bu)}{\partial s} + \frac{\partial (Bw)}{\partial z} = 0 \tag{7}$$

$$\frac{\partial c}{\partial t} + u\frac{\partial c}{\partial s} + w\frac{\partial c}{\partial z} = \frac{1}{BReSc}\left[\frac{\partial}{\partial s}\left(BD\frac{\partial c}{\partial s}\right) + \frac{\partial}{\partial z}\left(BD\frac{\partial c}{\partial z}\right)\right] \tag{8}$$

in which Re denotes the Reynolds number and Sc is the Schmidt number, which can be calculated from $Sc = \nu/D$, with $\nu = \mu/\rho$, where ν is the kinematic viscosity and μ is the dynamic viscosity. The unknowns u and w represent the mean longitudinal and vertical velocity components, respectively. If $\hat{\mathbf{v}} = \hat{u}\mathbf{i} + \hat{w}\mathbf{k}$ is the original velocity field and $\mathbf{v} = u\mathbf{i} + w\mathbf{k}$ is the laterally averaged velocity field, the components of $\mathbf{v}$ are obtained by

$$u = \frac{1}{B}\int_0^B \hat{u} db \tag{9}$$

$$w = \frac{1}{B}\int_0^B \hat{w} db \tag{10}$$

Similarly, the averaged concentration scalar field is given by

$$c = \frac{1}{B}\int_0^B \hat{c} db \tag{11}$$

The stresses that appear in the second term of the right side of Eq. (5) and Eq. (6) are the shear stresses in left and right margins of the reservoir in s and z directions. Considering newtonian fluid model for an incompressible fluid, the stress tensor can be expressed as

$$\underline{\mathrm{T}} = -p\underline{1} + \mu\left[\nabla\mathbf{v} + (\nabla\mathbf{v})^T\right] \tag{12}$$

where p stands for the laterally averaged pressure field. Since viscosity is assumed to be constant, we have that

$$\nabla\cdot(\nabla\mathbf{v})^T = \nabla(\nabla\cdot\mathbf{v}) = 0 \tag{13}$$

This relation, together with Eq. (12), allows us to rewrite Eq. (5) and Eq. (6) as

$$B\left(\frac{\partial u}{\partial t} + u\frac{\partial u}{\partial s} + w\frac{\partial u}{\partial z}\right) = \frac{\nu}{Re}\left[\frac{\partial}{\partial s}\left(B\frac{\partial u}{\partial s}\right) + \frac{\partial}{\partial z}\left(B\frac{\partial w}{\partial s}\right)\right] + \frac{1}{\rho}\left(\tau_s^L + \tau_s^R\right) \tag{14}$$

$$B\left(\frac{\partial w}{\partial t} + u\frac{\partial w}{\partial s} + w\frac{\partial w}{\partial z}\right) = -\frac{1}{\rho}\frac{\partial(Bp)}{\partial z} + \frac{\nu}{Re}\left[\frac{\partial}{\partial z}\left(B\frac{\partial u}{\partial z}\right) + \frac{\partial}{\partial s}\left(B\frac{\partial w}{\partial z}\right)\right] + \frac{1}{\rho}\left(\tau_z^L + \tau_z^R\right) + Bg \tag{15}$$

Note that the equations were both multiplied by B.

3. NUMERICAL FORMULATION

To solve the system of equations the Finite Element Method (FEM) is employed. Suppose that Eq. (14), Eq. (15), Eq. (7) and Eq. (8) are defined in a domain Ω and let S be the subspace defined by

$$S = \mathcal{H}^1(\Omega)^m = \left\{\mathbf{v} = (v_1, ..., v_m) | v_i \in \mathcal{H}^1(\Omega), \forall\, i = 1, ..., m\right\} \tag{16}$$

where $\mathcal{H}^1(\Omega)$ is the Sobolev space of functions and first order derivative functions square integrable over Ω. Let $L^2(\Omega)$ be a space of infinite dimension so that

$$L^2(\Omega) = \left\{v : \Omega \to \mathbb{R} \mid \int_\Omega v^2 d\Omega < \infty\right\} \tag{17}$$

Introducing the weight functions $\mathbf{w}$, q and r, the FEM implementation consists on finding solutions $\mathbf{v} \in S$, $p \in L^2$ and $c \in L^2$ such that

$$\int_\Omega B\frac{D\mathbf{v}}{Dt}\cdot\mathbf{w}d\Omega + \frac{1}{\rho}\int_\Omega Bp(\nabla\cdot\mathbf{w})d\Omega + \nu\int_\Omega B\nabla\mathbf{v}:\nabla\mathbf{w}d\Omega - \frac{1}{\rho}\int_\Gamma\left(\tau^L + \tau^R\right)(\mathbf{w}\cdot\mathbf{n})d\Gamma - \int_\Omega B\mathbf{g}\cdot\mathbf{w} = 0 \tag{18}$$

$$\int_\Omega(\nabla\cdot\mathbf{v})Bqd\Omega = 0 \tag{19}$$

$$\int_\Omega B\frac{Dc}{Dt}rd\Omega + \frac{1}{ReSc}\int_\Omega(BD\nabla c)\cdot\nabla rd\Omega = 0 \tag{20}$$

where ∇ denotes 2d divergent and gradient operators. In Eq. (18), τ^L and τ^R are left and right shear stress vectors, and the operator (:) is the tensor inner product. The Semi-discrete Galerkin method is employed for discretization of Eq. (18),

Eq. (19) and Eq. (20), in which time derivatives remain continue. According to this method, the domain Ω is discretized in a triangular finite element mesh. The unknowns u, w, p and c are approximated by

$$\hat{u}(s,z,t) \approx \sum_{N_u} N_n^u(s,z)u_n(t) \tag{21}$$

$$\hat{w}(s,z,t) \approx \sum_{N_w} N_n^w(s,z)w_n(t) \tag{22}$$

$$\hat{p}(s,z,t) \approx \sum_{N_p} N_n^p(s,z)p_n(t) \tag{23}$$

$$\hat{c}(s,z,t) \approx \sum_{N_c} N_n^c(s,z)c_n(t) \tag{24}$$

where N_n^u, N_n^w, N_n^p and N_n^c are the so-called shape functions for evaluation of the unknowns at each node n, and the node value of each unknown is represented by u_n, w_n, p_n and c_n. The number of nodes of velocity components, pressure and scalar are denote by N_u, N_w, N_p and N_c. The application of FEM consists of solving the system composed by Eq. (18), Eq. (19) and Eq. (20) in the domain of each element (Ω_e). Integrations of each term over Ω_e for all elements yield

$$M_s\dot{u} + \frac{1}{BRe}\left[\left(2K_{ss} + K_{zz}\right)u + K_{sz}w\right] + \frac{g}{B}G_sBp = 0 \tag{25}$$

$$M_z\dot{w} + \frac{1}{BRe}\left[K_{zs}u + \left(K_{ss} + 2K_{zz}\right)w\right] + \frac{g}{B}G_zBp = 0 \tag{26}$$

$$D_su + D_zw = 0 \tag{27}$$

$$M_c\dot{c} + \frac{1}{ReSc}\left(K_{ss} + K_{zz}\right)c = 0 \tag{28}$$

Note that the substantive derivatives of velocity components and scalar are respectively represented by $\dot{u}$, $\dot{w}$, and $\dot{c}$, which are responsible for advection effects, and are time discretized by a Semi-Lagrangian scheme. This approach allows the use of large time steps without limiting the stability, in contrast to the Eulerian framework. The choice of the time step is only limited by numerical accuracy, since instabilities appear when trajectories cross and particles "overtake" others. If $\triangle t$ is a finite time difference, the Semi-Lagrangian scheme approximates the substantive derivatives in a time step $m+1$ in the node n by

$$\frac{D\mathbf{v}_n}{Dt} \approx \frac{\mathbf{v}_n^{m+1} - \mathbf{v}_d^m}{\triangle t} \tag{29}$$

$$\frac{Dc_n}{Dt} \approx \frac{c_n^{m+1} - c_d^m}{\triangle t} \tag{30}$$

where the subscript d (from departure) refers to the element from which the particle came. Time and spatial discretization of Eq. (25), Eq. (26) and Eq. (27) give rise to an algebraic linear system in the form

$$\begin{bmatrix} B & -\triangle tG \\ D & 0 \end{bmatrix}\begin{bmatrix} \mathbf{v}^{m+1} \\ p^{m+1} \end{bmatrix} = \begin{bmatrix} a_{\mathbf{v}}^{m+1} \\ a_p^{m+1} \end{bmatrix} \tag{31}$$

Matrices B, D and G are given by

$$B = M + \frac{\triangle t}{Re}K \tag{32}$$

$$D = \begin{bmatrix} D_s & 0 \\ 0 & D_z \end{bmatrix} \tag{33}$$

$$G = \begin{bmatrix} G_s & 0 \\ 0 & G_z \end{bmatrix} \tag{34}$$

and, in Eq. (32), matrices M and K are

$$M = \begin{bmatrix} M_s & 0 \\ 0 & M_z \end{bmatrix} \tag{35}$$

$$K = \begin{bmatrix} 2K_{ss} & K_{zs} \\ K_{sz} & 2K_{zz} \end{bmatrix} \tag{36}$$

The solution of Eq. (31) is obtained by means of the Projection Method, while Eq. (28) is solved separately.

4. MESH GENERATION

In order to capture the hydrodynamic and thermal processes along the reservoir depth by a two-dimensional approach the finite element mesh must be a vertical mesh, along a certain horizontal path. The algorithm for mesh generation was designed for complex terrain geometries combined with hydrographic maps. Topological data are obtained from a set of level curves that provides the reservoir bottom coordinates and the width at each point of the vertical mesh, while the hydrographic maps provides the horizontal (or longitudinal) direction. These maps contain the coordinates associated to the riverbed, where we believe that hydrodynamic effects will be more significant.

The next figure shows a top view, in the left side, of the terrain data for a selected region combined with the hydrographic map, and, in the right side, the riverbed line (longitudinal direction). The vertical mesh – referred to as 2dw mesh – will be generated above the riverbed (highlighted blue line), which provides bottom coordinates. The orange lines represent the reservoir margins and are used in the calculation of the width.

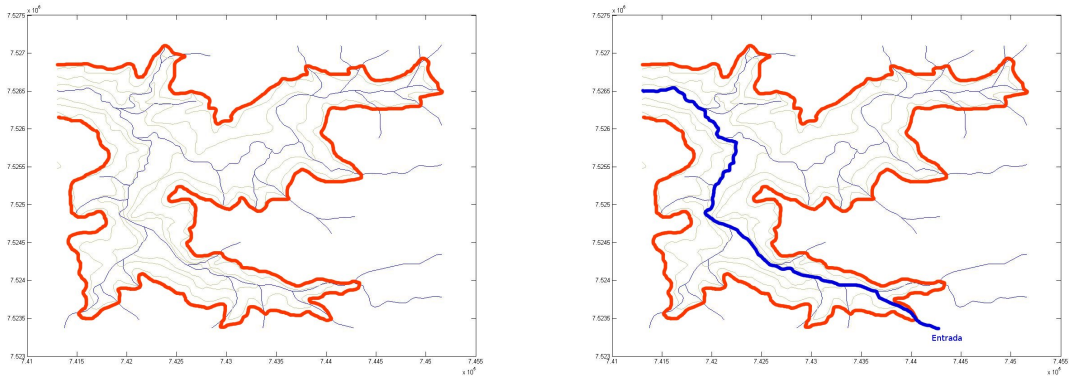

Figure 1. Superposition of terrain and hydrographic data

After gathering the necessary information, the first stage is the triangulation on the terrain data [Dongala *et al*., 2006], to generate the terrain mesh (not the vertical mesh yet). This step allows the interpolation of terrain coordinates at any point of the reservoir, which will be useful for bottom and width calculations. The second step consists on projecting the riverbed line on the reservoir bottom. Now, the vertical triangulation can be performed to assemble the vertical mesh (third step). The next figures illustrate the process.

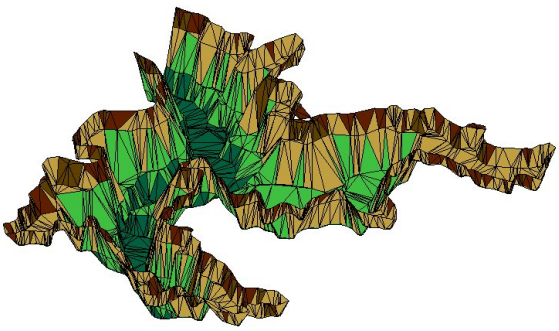

Figure 2. Terrain mesh

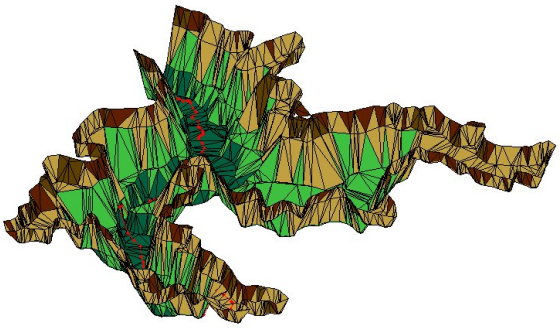

Figure 3. Terrain mesh and projected riverbed

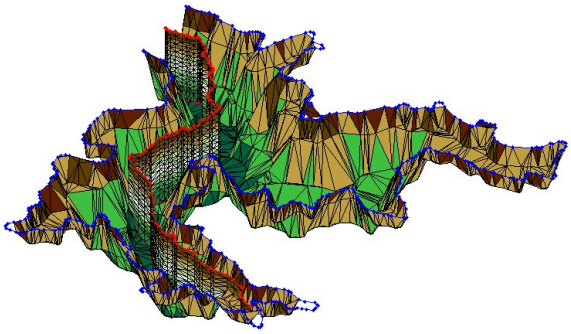

Figure 4. Superposition of terrain mesh and vertical mesh

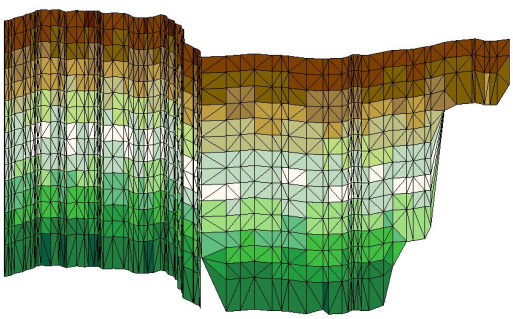

Figure 5. Vertical mesh (2dw mesh)

The calculation of the width for each point of the 2dw mesh can now be performed. In the presented model, each width B_n associated to node n is the sum of the distance from the node to left side, B_n^L, and to the right side, B_n^R. That is,

$$B_n = B_n^L + B_n^R \tag{37}$$

This procedure is shown in the following figure.

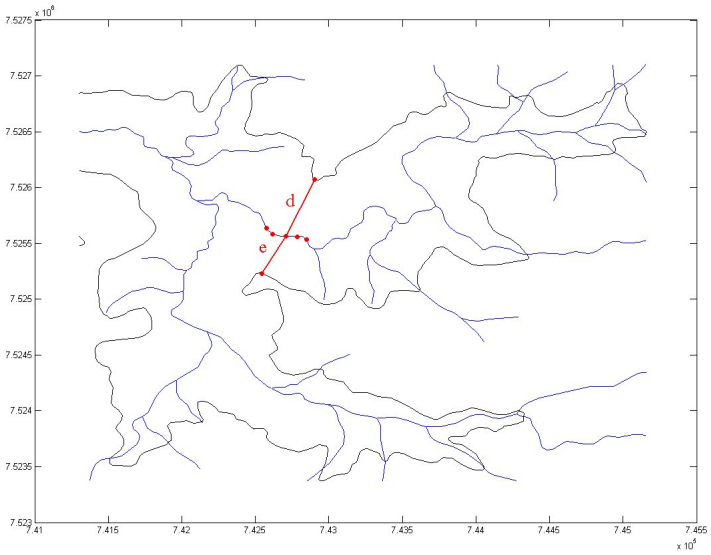

Figure 6. Width calculation

5. CODE VALIDATION

To validate the model and the code, an experimental simulation of a density current problem [Paterson *et al.*, 2005] was carried out, since this is predominantly a 2d depth dependent problem. A flume was filled with two fluids of different densities ρ: one half with a solution of salt in water ($\rho = 1020Kg/m^3$) and the other with water ($\rho = 980Kg/m^3$). The heavier fluid also received an amount of sodium permanganate ($NaMnO_4$) as tracer. The two fluids were initially separate, until the sudden removal of the separator. In the following figures synchronized frames of experimental and simulation processes are shown for each instant t.

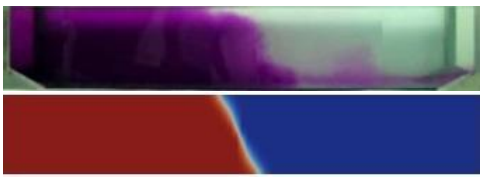

Figure 7. $t = 2s$

Figure 8. $t = 3s$

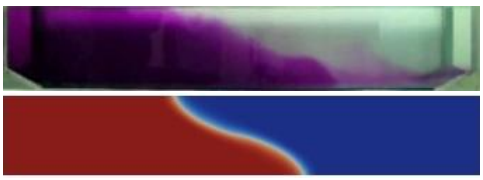

Figure 9. $t = 5s$

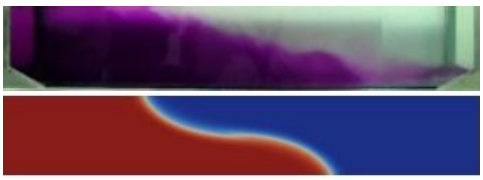

Figure 10. $t = 7s$

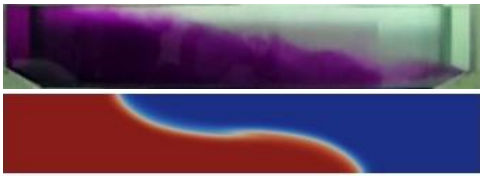

Figure 11. $t = 9s$

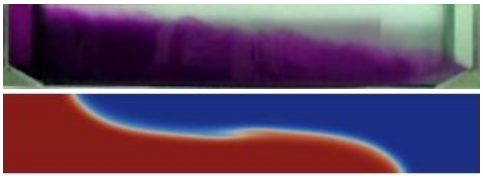

Figure 12. $t = 12s$

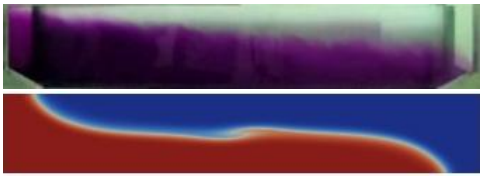

Figure 13. $t = 15s$

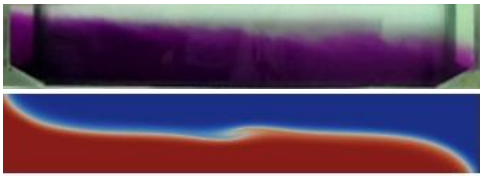

Figure 14. $t = 17s$

Although without a turbulence model, the simulation showed good timing results. The mixing profile can be improved by mesh refinement, since the code took only approximately 20 minutes to reach time $t = 17s$.

6. RESERVOIR SIMULATION

In this section, numerical results of a reservoir simulation are reported, employing the mesh shown by Fig.5. The domain length is 2,700m, with 80m of depth. Water inflow carries a certain solute concentration into the reservoir, with 1m/s as inflow velocity (this is a typical value). The following figures show the solution of the scalar field at four different times t. The vertical mesh simulation is presented in the longitudinal-vertical plane.

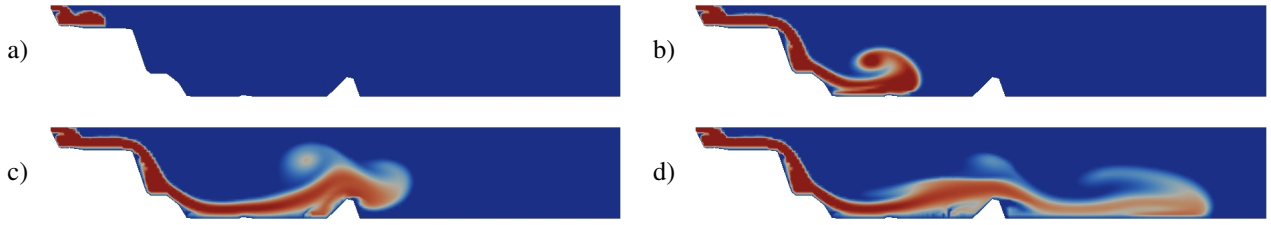

Figure 15. (a) $t = 13min$; (b) $t = 67min$; (c) $t = 133min$; (d) $t = 200min$.

It can be seen by the results that the density gradient tends to keep the heavier fluid in the bottom, forming a stratified configuration. Additionally, some vortices are originated by the flow, as shown in Fig.16.

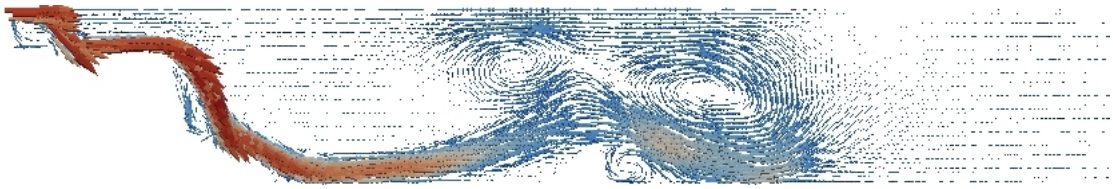

Figure 16. Velocity field.

7. CONCLUSION

Computational code tests and experimental validation showed that the model is capable to simulate important depth dependent environmental phenomena associated to hydroelectric reservoir for many analysis. All reservoir simulations employing the 2dw model took less than 60 minutes to provide significant information, one order of magnitude less than a 3d simulation of the same problem. The low computational cost allows the use of very fine meshes, enhancing the quality of numerical results. The laterally averaged model (2dw) and depth averaged model (2dh)– widely used in shallow water simulations [Rosman, 2001] – are complementary models, which means that one can obtain satisfactory information by combining 2dw and 2dh simulations, without the computational penalty of a heavy 3D simulation. The tool presented in this paper also counts with a complete GUI (Graphical User Interface), where the user can manipulate all terrain, hydrographic and mesh data, making the simulation set up easier.

8. ACKNOWLEDGEMENTS

We thank Promon Engenharia for financial and technical support and CNPq and FAPERJ for financial support.

9. REFERENCES

Dongala, A.M., Lima, L.M.R., Mangiavacchi, N., Soares, C.B.P., 2006, "Finite element mesh generation for numerical simulation of hydroelectric power plant reservoir filling", Proceedings of the 11th Brazilian Congress of Thermal Sciences and Engineering, Curitiba, Brazil, pp. 41-44.

Jorgensen, S.E., 1979, "Handbook of Environmental and Ecological Parameters", Pergamon Press, Oxford.

Karpik, S.R., Raithby, G.D., 1990, "Laterally Averaged Hydrodynamics Model For Reservoir Predictions", Journal of Hydraulic Engineering, Vol. 116, No. 6.

Paterson, M.D., Simpson, J.E., Dalziel, S.B., Nikiforakis, N., 2005, "Numerical Modeling of Two-dimensional and Axis-symmetric Gravity Currents", International Journal for Numerical Methods in Fluids, Vol. 47, pp. 1221-1227.

Rosman, P.C.C., 2001, "Um Sistema Computacional de Hidrodinâmica Ambiental", in Silva, R.C.V., "Métodos Numéricos em Recursos Hídricos 5.1", Ed. Porto Alegre: ABRH, Vol. 5, pp. 1-161.